Mechanism of hydrocarbon reduction using multiple injection in a natural gas fuelled/micro-pilot diesel ignition engine

G J Micklow and **W Gong**
The University of North Carolina, Charlotte, North Carolina, USA

Received 25 January 2002

Abstract: *Research has shown that a large amount of natural gas (NG) is unburned at light loads in an NG fuelled/micro-pilot diesel compression ignition engine. A mechanism of unburned hydrocarbon (HC) reduction using multiple injections of micro-pilot diesel has been proposed in this paper. Multidimensional computations were carried out for a dual-fuel engine based on a modified CAT3401 engine configuration. The computations show that a split injection with a small percentage (e.g. 30 per cent of diesel in the second injection pulse) can significantly reduce HC, CO and* NO_x *emissions. Based on parametric studies to optimize the timing of both of the injection pulses, HC emissions could be reduced by 90 per cent, with a reduction in CO emissions of 50 per cent and* NO_x *emissions of 70 per cent in comparison to a single-injection pulse-base case configuration.*

Key words: *HC reduction, multiple injection, NG fuelled/micro-pilot diesel ignition engine*

1. Introduction

The combustion technique for a micro-pilot ignition dual-fuel engine, in which a mixture of gaseous fuel and air is compressed to a point below the self-ignition temperature and then ignited by the injection of a small quantity of diesel fuel or a spark, has been used for a considerable time. The increase in availability of diesel fuel and the advances in compression ignition (CI) engine technology during the middle third of the twentieth century reduced the popularity of the dual-fuel engine [**1**]. However, the development of the technology required to operate transportation vehicles on alternative fuels resumed in direct response to the energy crises of the 1970s [**2**]. The near-term driver since the 1990s is the requirement to comply with the more and more stringent emissions standards. Among various alternative fuels (other than diesel and gasoline), natural gas is widely used in many ground-based gas turbine and CI engine applications due to its ready availability, low-cost and clean-burning attributes. The main constituent of natural gas, methane, has good knock-resistant qualities that make it an excellent fuel for high compression ratio engine applications. Many researchers have studied the performance of the homogeneous charge compression ignition (HCCI) engine configurations [**3**, **4**]. In HCCI engines, a homogeneous mixture of a gaseous fuel and air is introduced into the cylinder in a similar way to spark ignited gasoline engines. While HCCI engines can operate at near stoichiometric conditions with a relatively high flame temperature similar to gasoline engines, HCCI engines are normally operated at part load with diluted homogeneous mixtures. Thus, unlike gasoline engines where high NO_x production is found at high flame temperatures or diesel engines in which high soot is formed from fuel-rich regions and high NO_x is formed from high-temperature regions, the lean operation of HCCI engines results in lower flame temperatures with lower NO_x production and negligible soot formation [**4**].

However, there are still challenges associated with the successful operation of HCCI engines. One of them is the relatively poor light load and idling performance associated with low efficiency and potentially inferior emission characteristics [**5**, **6**]. The extent of this deterioration in performance depends largely on the

JER 00302 · © 2002 · IMechE

composition of the gaseous fuel being used and the engine employed [6]. Another cause may be the low concentration of the gaseous fuel, which results in a low flame speed [7], which may be quenched before complete combustion is achieved. Thus, much of the methane can remain unburned, surviving to the exhaust stage. Therefore, the natural gas–air ratio in an HCCI engine is an important consideration. If the fuel––air ratio is reduced below the lean flammability limit, the engine will misfire. Even though the direct injected pilot will operate without misfire with mixtures as lean as an equivalence ratio, ϕ, of 0.25, the practical range of ϕ for acceptable combustion is above 0.5 [8]. A similar equivalence ratio is also recommended in reference [1]. In order to maintain proper fuel–air ratios, the air charge must be throttled at light loads, which increases pumping losses thereby lowering efficiency. Researchers have tried to find alternative methods to enhance the efficiency of the gas exchange, by late intake valve closing (IVC) [9] and a hydraulic variable valve timing system [10], among others. These systems have resulted in increases in engine efficiency. However, these systems have to accommodate the conflicting requirement of the optimum valve timing at full loads and light loads, and late IVC also reduces the effective actual compression ratio with negative effects on performance and efficiency. Other methods are to extend the lower limit boundary to lower gaseous concentrations in the air charge through the employment of a number of procedures, such as using a larger amount of pilot diesel along with higher inlet temperatures at light loads [6] or adding a small amount of higher hydrocarbon components (butane and heavier) [11], etc. However, the inlet temperature is restricted by both knocking and NO_x emissions and the effect of using large amounts of pilot diesel is also limited.

With development of the electronically driven micro-pilot diesel system [8], it is possible to issue multiple injections of diesel at light loads. The diesel injected into the cylinder by the first pulse acts as the added 'higher hydrocarbon' constituent which will ignite weakly before NG ignition. This can increase the mixture temperature before ignition and extends the lower limit of flammability. Then, the mixture of natural gas and air is ignited by the second diesel injection pulse. This paper will investigate the effect of this concept at various running conditions.

2. Computational Technique and Model Description

The program used in the current study is the KIVA3V code [12] originally developed by the Los Alamos National Laboratory. The standard KIVA code was modified to enable dual-fuel combustion modelling. In the simulations, it is assumed that a homogeneous mixture has been reached at the beginning of the computation, i.e. intake valve closure (IVC).

3. Combustion Model

In general, computer time and storage constraints place severe restrictions on the complexity of the reaction mechanisms that can be accommodated in numerical simulations of combustion systems. Detailed mechanisms and rate coefficients for chemical reactions of practical interest are often uncertain so multidimensional reactive flow calculations typically use simplified chemical kinetic schemes in which the reactions of interest are represented by a manageably small number of reaction steps involving a small number of reaction species [13–15]. Overall kinetic schemes attempt to simplify the chemistry in order to predict important physical quantities while maintaining computational efficiency. These quantities include the in-cylinder pressure and temperature, and the concentration of important species such as fuel, CO, CO_2, H_2 and H_2O.

The combustion process in an NG fuelled engine, ignited by pilot diesel, includes diesel combustion and natural gas combustion. The diesel combustion employs an overall one-step scheme

$$\text{Diesel} + n_1 O_2 \rightarrow n_2 CO_2 + n_3 H_2O \tag{1}$$

where n_1, n_2 and n_3 are the coefficients to balance the reaction.

Previous studies by the authors have found that a one-step scheme for the methane combustion cannot predict the CO emissions. Therefore, the combustion of natural gas (methane) uses the following two-step reaction scheme:

$$CH_4 + 1.5O_2 = CO + 2H_2O \tag{2}$$

$$CO + 0.5O_2 = CO_2 \tag{3}$$

The reaction rates are given by

$$\frac{d}{dt}[CH_4] = -2.8 \times 10^9 [CH_4]^{-0.3}[O_2]^{1.3} \times \exp\left(-\frac{48.4}{RT}\right) \tag{4}$$

$$\frac{d}{dt}[CO] = -3.98 \times 10^{14}[CO]^{1.0}[H_2O]^{0.5} \times \exp\left(-\frac{40.0}{RT}\right) + 5.0 \times 10^{8}[CO_2]^{1.0} \times \exp\left(-\frac{40.0}{RT}\right) \tag{5}$$

The units of the universal gas constant R are kcal/gmol K. The rate coefficients for equations (4) and (5) are taken from Westbrock and Dryer [**16**] and Dryer and Glassman [**17**].

Five equilibrium reactions are considered:

$$H_2 \leftrightarrow 2H \tag{6}$$

$$O_2 \leftrightarrow 2O \tag{7}$$

$$N_2 \leftrightarrow 2N \tag{8}$$

$$O_2 + H_2 \leftrightarrow 2OH \tag{9}$$

$$O_2 + 2H_2O \leftrightarrow 4OH \tag{10}$$

The sixth equilibrium reaction

$$O_2 + 2CO \leftrightarrow 2CO_2 \tag{11}$$

in the standard KIVA3V code is dropped in order to obtain a good prediction of CO for the dual-fuel case.

4. NO_x Model

While nitric oxide (NO) and nitrogen dioxide (NO_2) are usually grouped together as NO_x emissions, nitric oxide is the predominant oxide of nitrogen produced inside the engine cylinder [**15**]. The extended Zeldovich mechanism is employed for NO formation:

$$O + N_2 \leftrightarrow NO + N \tag{12}$$

$$N + O_2 \leftrightarrow NO + O \tag{13}$$

$$N + OH \leftrightarrow NO + H \tag{14}$$

5. Computational Grids

The grid used in this study is shown in Fig. 1. The computational geometry includes a moving piston with an axisymmetrical Mexican hat piston bowl and the cylinder. Since the injector of this engine is located at the centre of the cylinder and its six orifices are equally spaced, a 60° sector mesh (i.e. sector symmetry was assumed to save computer time) with 30 cells in the radial direction, 20 cells in the azimuthal direction and 25 cells in the z direction was employed.

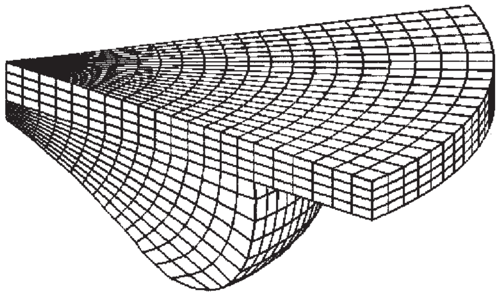

Fig. 1 *Grid for the engine simulation.*

6. Engine Simulation Results

The predictions obtained by the models described above are compared with the experimental results. The engine specifications, initial/boundary and operating conditions are outlined in Tables 1 and 2.

Figure 2 shows the comparison between predicted and measured in-cylinder pressure. Reaction rates were adjusted in order to achieve good agreement. The predicted emissions for the baseline case are compared with measure values in Table 3. It is apparent that the emissions are well predicted without any adjustment for the baseline case. This gives confidence to further investigate methods to reduce emissions at light loads in dual-fuel engines.

Figure 3 shows the in-cylinder methane mass history. It is apparent that almost 40 per cent of methane is unburned and very little methane can be burned after a crankshaft angle (CA) of 420°. The methane mass distribution of a CA of 433° is shown in Fig. 4. Most of the unburned methane is in the vicinity of

Bore (mm) × stroke (mm)	137.6 × 165.1
Connecting rod (mm)	261.62
Compression ratio	15.1
Number of nozzle orifices	6
Fuel	$C_{14}H_{30}$
Initial swirl ratio	0.978
Cylinder wall temperature (K)	433
Cylinder head temperature (K)	523
Piston face temperature (K)	553
Displacement volume (L)	2.44
Spray angle (from cylinder head)	27.5°

Table 1 Engine specifications and operating conditions.

Energy supplied by NG (%)	85
Equivalent ratio of NG	0.33
Inlet temperature (K)	348
Inlet pressure (kPa)	151
Injection timing (°CA BTDC)	30
Load (%)	50
Speed (r/min)	1700
Brake power (kW)	21

Table 2 The specification of the cases studied.

JER 00302

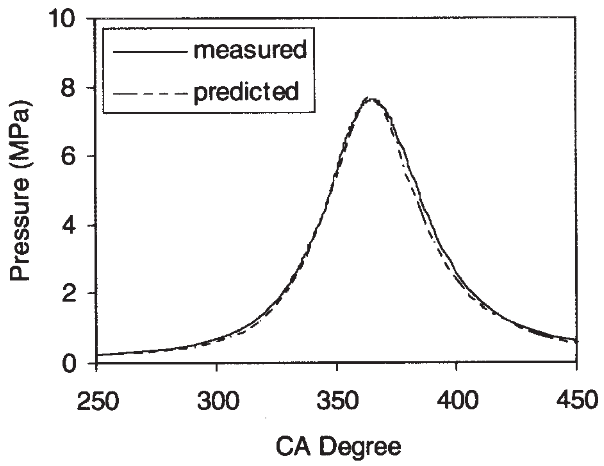

Fig. 2 *In-cylinder pressure at half load, 1700 r/min, 85 per cent energy supplied by NG.*

	HC (ppm)	CO (ppm)	NO_x (ppm)
Measured	13601	2408	145
Predicted	14490	2264	87

Table 3 Comparison of measured and predicted emissions.

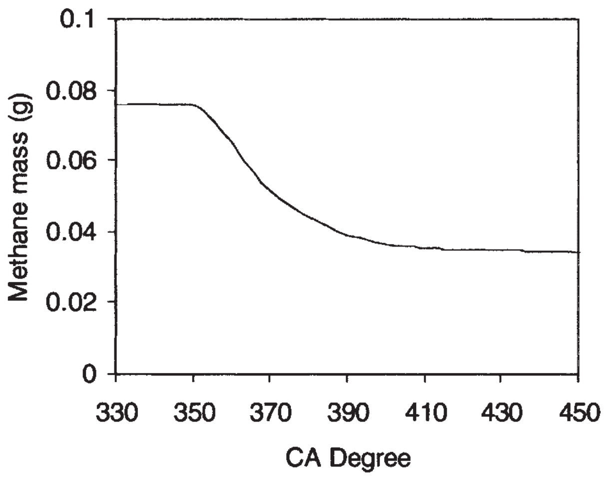

Fig. 3 *Methane mass history in cylinder, 85 per cent energy supplied by natural gas at half load, 1700 r/min.*

the cylinder wall. Figure 5 illustrates the cause of this problem. When the micro-pilot diesel is injected into the cylinder late in the compression stroke, few diesel droplets can reach the squish area. Although the methane–air mixture in the piston bowl is ignited by diesel successfully, the flame cannot propagate into the squish area due to the slow flame speed in the extreme lean mixture. Furthermore, the flame is also easy to quench by the low wall temperature in the lean mixture.

The purpose of the split injection is to increase the amount of diesel vapour in the squish area. A specified percentage (e.g. 67 per cent) of the total amount

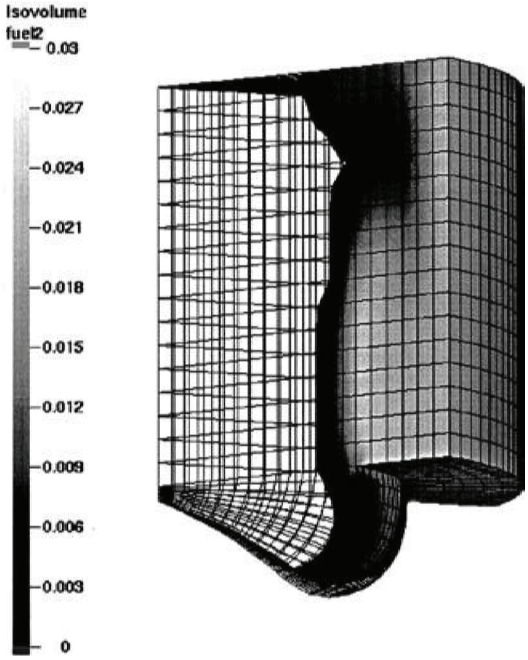

Fig. 4 *Unburned methane at 433° CA, 85 per cent energy supplied by natural gas at half load, 1700 r/min, single injection.*

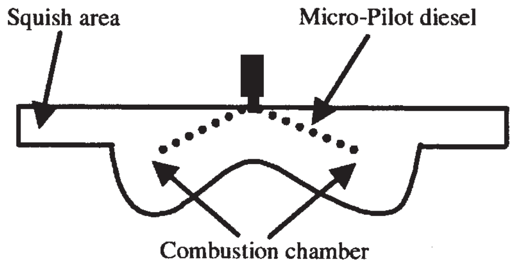

Fig. 5 *Illustration of cause of the problem shown in Fig. 4.*

of pilot diesel is injected into the cylinder in the first pulse at the middle of the compression stroke, as shown in Fig. 6a. The temperature in the cylinder is relatively low at this time. Therefore, diesel droplets evaporate slowly and can reach the vicinity of the cylinder wall easily. As the piston approaches top dead centre (TDC), the diesel injected in the first pulse is mixed with air in the squish area. Since the activation energy of diesel oxidation is lower than that in methane oxidation, the temperature in the squish area is increased due to diesel oxidation. Such an effect is similar to increasing the inlet temperature. Since only a small amount of diesel is injected in the homogeneous charge compression ignition (HCCI) engine, a very lean and homogeneous diesel–air mixture is formed when reactions start. Therefore, the temperature increase due to the reaction between diesel injected in the first pulse and air is not high enough to ignite the natural gas mixture. The second injection pulse is needed to ignite the natural gas mixture late in the compression stroke,

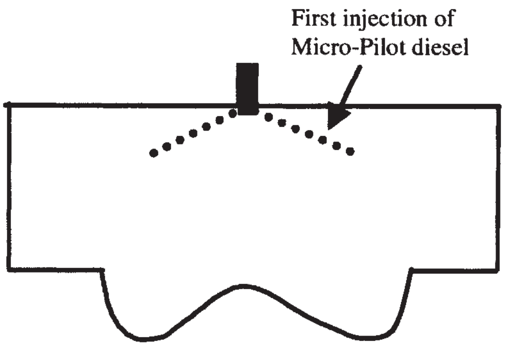

(a) The first pulse in the middle of the compression stroke

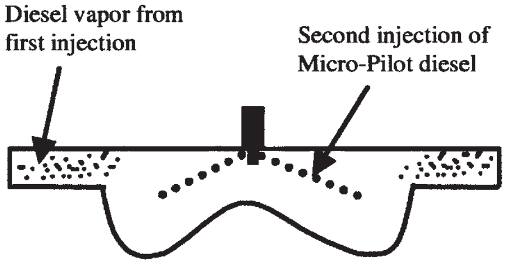

(b) The second pulse in the middle of the compression stroke

Fig. 6 *Illustration of multiple injections.*

as shown in Fig. 6b. The baseline case for multiple injections is outlined in Table 4.

Figures 7 to 10 show the effect of the injection timing of the first pulse on power and emissions. All conditions are the same as those in the baseline case outlined in Table 4 except for the injection timing of the first pulse. The energy release shown in Fig. 7 is the total energy released from all chemical reactions up to a CA of 500°. The reason for the increased total energy in the multiple injections case is that more methane is burned, as shown in Fig. 8. Both HC and CO are significantly reduced when the first pulse injection timing is near a CA of 250°. If diesel is injected too early, many diesel droplets reach the cylinder wall and therefore cannot be mixed well with the air, while if the diesel is injected too late, fewer

Energy supplied by NG (%)	85
Equivalent ratio of NG	0.33
Inlet temperature (K)	348
Inlet pressure (kPa)	151
Amount of diesel in the first pulse	2/3 of total pilot diesel
Injection timing of the first pulse	250 ° CA
Amount of diesel in the second pulse	1/3 of total pilot diesel
Injection timing of the second pulse	330 ° CA
Speed (r/min)	1700

Table 4 Running conditions in the baseline case for the split injection mode in the dual-fuel case.

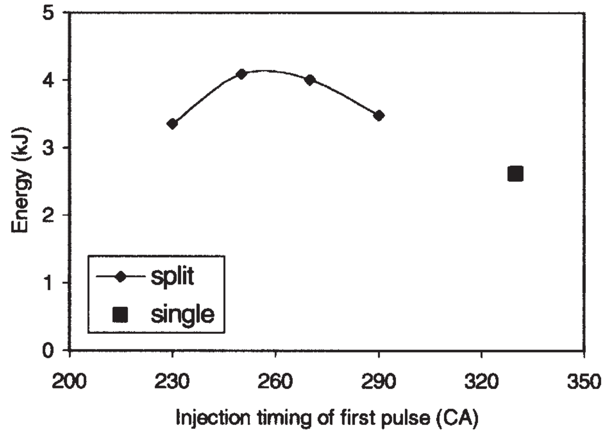

Fig. 7 *Effect of injection timing of the first pulse on energy released up to 500° CA: $\phi_{NG} = 0.33$, 1700 r/min.*

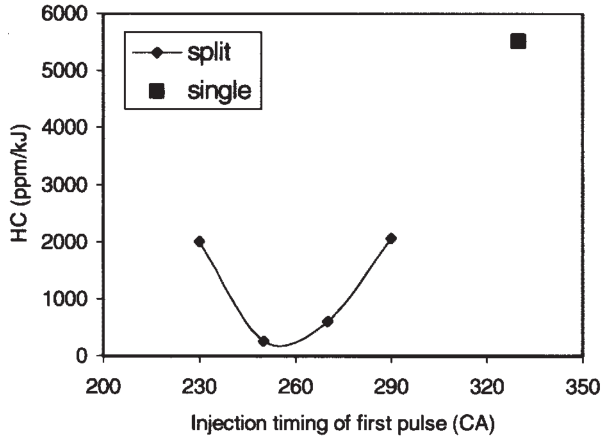

Fig. 8 *Effect of injection timing of the first pulse on HC emission: $\phi_{NG} = 0.33$, 1700 r/min.*

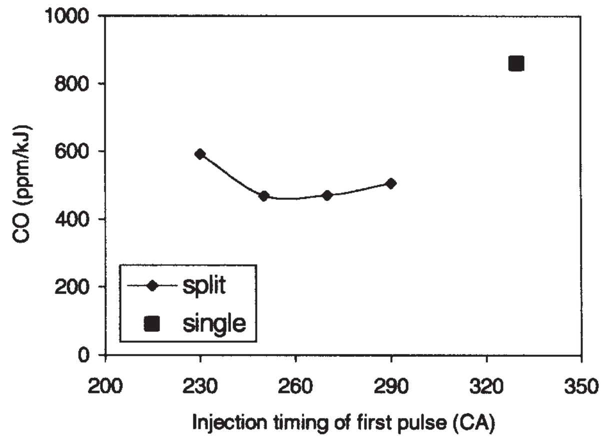

Fig. 9 *Effect of injection timing of the first pulse on CO emission: $\phi_{NG} = 0.33$, 1700 r/min.*

diesel droplets can reach the squish area. It is interesting to note that NO_x emission is also reduced by multiple injections. The reason is that most NO_x production in dual-fuel engines comes from the combustion of the micro-pilot diesel. Most of the diesel fuel injected in the first pulse can be mixed homogeneously before it is ignited, and then it is burned

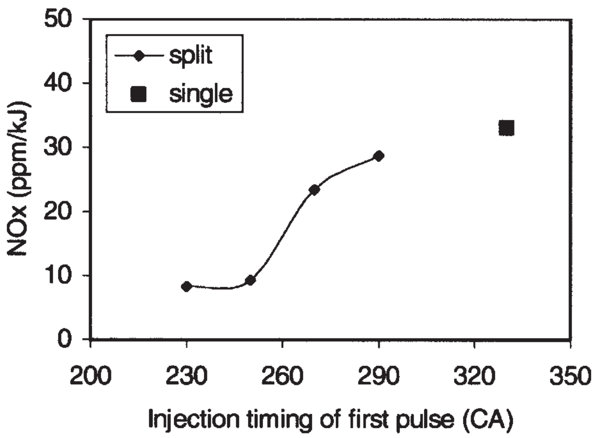

Fig. 10 *Effect of injection timing of the first pulse on* NO_x *emission:* $\phi_{NG} = 0.33$*, 1700 r/min.*

with the homogeneously lean mixture. The combustion temperature is low, which produces less NO_x. However, in the single injection mode, there is not enough time for the diesel to mix with all of the air in the cylinder, and most diesel is burned near stoichiometric conditions, which results in higher NO_x emissions. Similarly, when the injection timing of the first pulse is too late, i.e. 290° CA, there is not enough time for the diesel to mix with all the air in the cylinder to form a homogeneous lean mixture. A certain percentage of the diesel is burned near stoichiometric conditions or at a relatively rich mixture, which results in a higher combustion temperature and thus high NO_x emissions, compared to the case with an advanced injection timing, i.e. 250° CA.

Figure 11 shows the influence of injection timing of the first pulse on in-cylinder pressure. Split injection increases in-cylinder pressure, especially for late injection timing of the first pulse. At late injection timing of the first pulse, e.g. 290° CA, there is not enough time for the diesel injected during the first pulse to become homogeneously mixed with air and uniformly distributed in the cylinder. Therefore, a large percentage of the diesel fuel could be burned near the stoichiometric condition, which increases the maximum in-cylinder pressure. However, the increase is modest and is not thought to prohibit the use of this method.

Figure 12 shows the diesel mass history when the injection timing of the first pulse is at a CA of 250°. The total mass of diesel does not decrease until about a CA of 315°, which indicates that the temperature in the cylinder is not high enough to activate the oxidation of diesel before 315° CA. The evaporation rate is also very slow. Although reactions take place after 315° CA, the reaction rate is relatively low. Only after diesel of the second pulse is injected and ignition takes place at around 345° CA is the diesel fuel rapidly burned.

The methane mass fraction distribution obtained with split injection is shown in Fig. 13. Compared with Fig. 4, a marked reduction in unburned methane is observed.

Figures 14 to 16 show the effect of the second pulse injection timing on emissions. The first injection pulse timing is held fixed at a CA of 250°. From Fig. 14 it can be seen that a significant portion of the methane cannot be ignited if the second pulse injection timing is too early (e.g. 300° CA). The reason is that the diesel fuel injected in the second pulse has been mixed with the air and a lean mixture is formed before the in-cylinder temperature is high enough to activate the reaction of diesel and oxygen. Therefore, the combustion of the mixture is low and is not enough to ignite the natural gas mixture. Due to the same reason, the emissions of NO_x are also low, as shown in Fig. 15. Further, the injection timing of the second pulse cannot be too late, either. Otherwise,

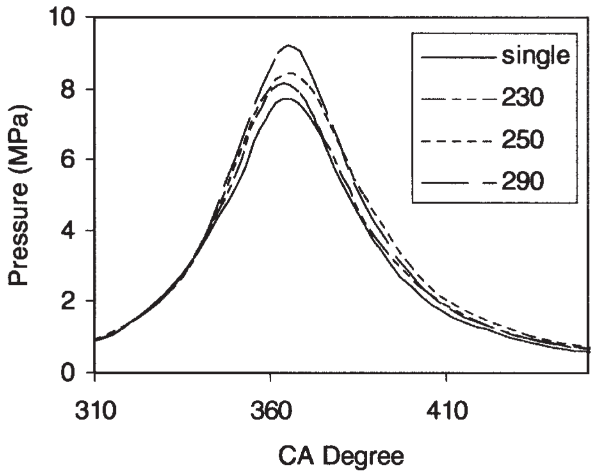

Fig. 11 *Effect of injection timing of the first pulse on in-cylinder pressure:* $\phi_{NG} = 0.33$*, 1700 r/min.*

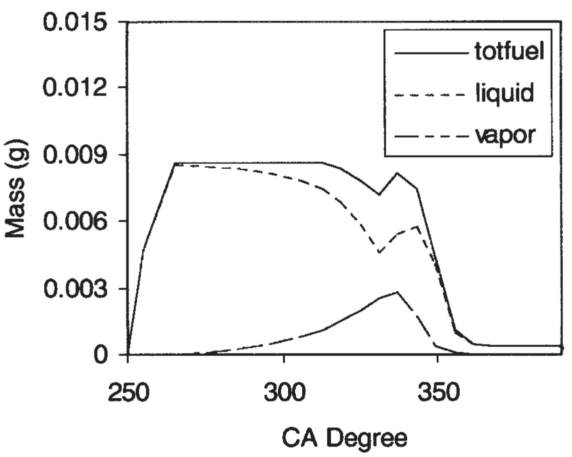

Fig. 12 *Diesel history:* $\phi_{NG} = 0.33$*, 1700 r/min, first pulse timing = 250° CA.*

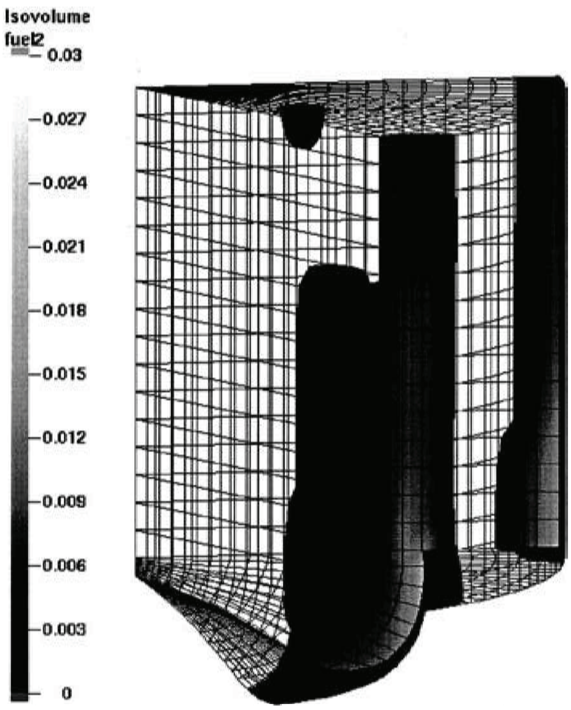

Fig. 13 *Unburned methane at 433° CA, ϕ_{NG}= 0.33, 1700 r/min, multiple injection, 250° CA for the first injection.*

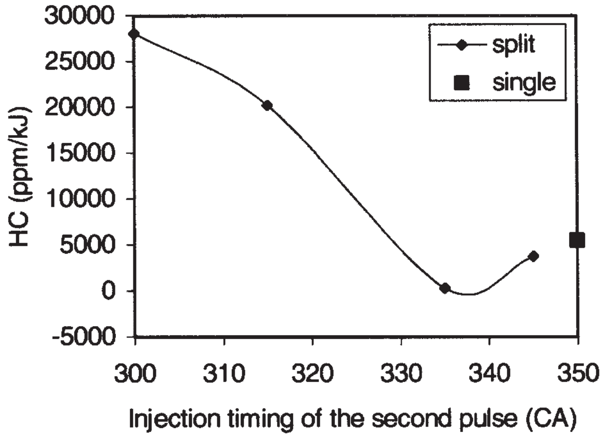

Fig. 14 *Effect of injection timing of the second pulse on HC emission: ϕ_{NG}= 0.33, 1700 r/min.*

there is not enough time to burn the natural gas completely. It is found from Fig. 14 that the optimal injection for the second pulse is at approximately 335° CA. After that, the unburned methane starts to increase as the injection timing is retarded. The optimal injection timing for CO emissions is also near 335° CA. CO emissions are increased when the injection timing is earlier or later than that point. However, a drop in the CO emissions is seen when the injection timing is advanced at a CA of 315°. This results from the fact that most methane is not ignited successfully and less CO is produced.

Figures 17 to 19 show the effect of the amount of diesel fuel injected for the second pulse on emissions.

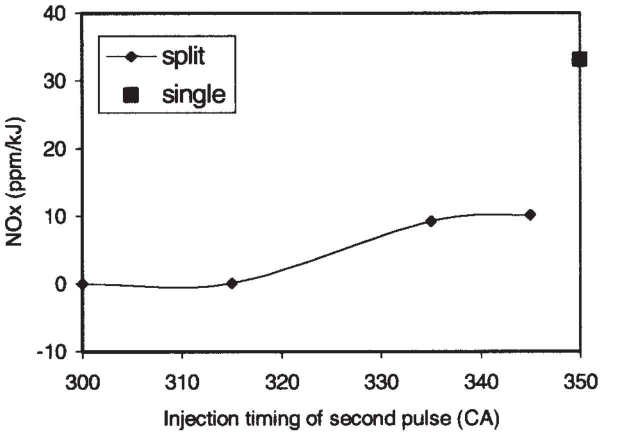

Fig. 15 *Effect of injection timing of the second pulse on NO_x emission: ϕ_{NG}= 0.33, 1700 r/min.*

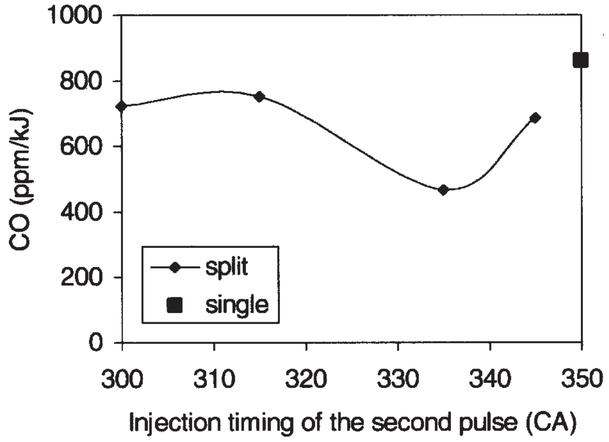

Fig. 16 *Effect of injection timing of the second pulse on CO emission: ϕ_{NG}= 0.33, 1700 r/min.*

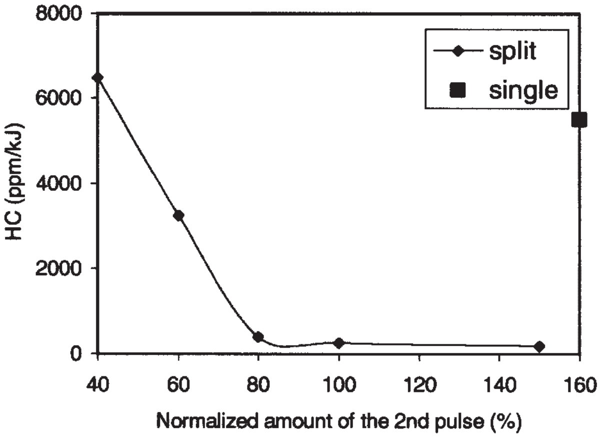

Fig. 17 *Effect of the amount of diesel fuel injected for the second pulse on HC emissions: ϕ_{NG}= 0.33, 1700 r/min.*

The first injection timing is maintained at 250° CA with the same amount of fuel injected as before. The amount of disel injected for the second pulse is normalized by the amount in the baseline split injection mode case. From Fig. 17, it can be seen that a rapid reduction in HC emissions occurs with increasing amounts of fuel injected. At approximately 80 per

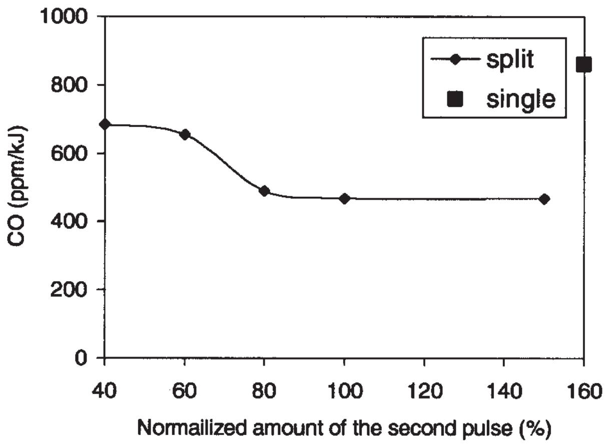

Fig. 18 *Effect of the amount of diesel fuel injected for the second pulse on CO emissions: ϕ_{NG}= 0.33, 1700 r/min.*

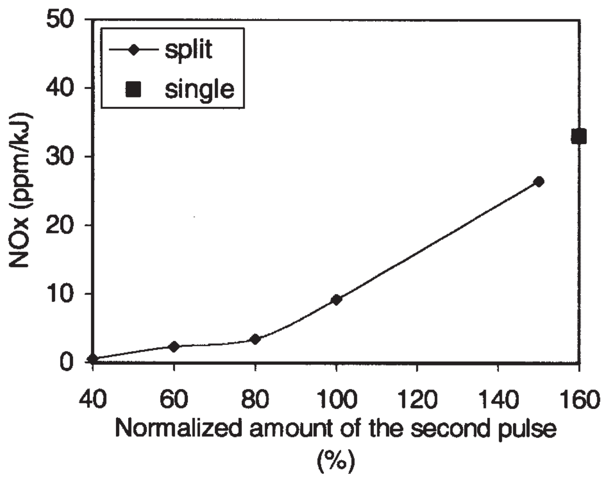

Fig. 19 *Effect of the amount of diesel fuel injected for the second pulse on NO_x emissions: ϕ_{NG}= 0.33, 1700 r/min.*

cent of the amount used in the baseline case, the HC and CO emissions become relatively constant at a very low level. Further increasing the amount of diesel fuel injected has little effect on the HC and CO emissions but NO_x emissions are significantly increased. Therefore, 80 per cent of the diesel fuel amount used in the baseline case is recommended.

Figures 20 to 22 show the effect of amounts of diesel fuel injected for the first pulse on emissions. The first injection timing is maintained at a CA of 250°. The second injection timing is at 335° CA and keeps the same baseline split injection mode amount. The amount of diesel fuel injected for the first pulse is normalized by the amount in the baseline case. From Fig. 20 it can be seen that amounts above 80 per cent of the diesel fuel injection amount used in the baseline case are required to reduce HC and CO to very low levels. Reduction in the amount of diesel fuel injected that is less than that results in a continuous increase in unburned methane. Further increasing the diesel amount has little effect on the HC and CO emissions.

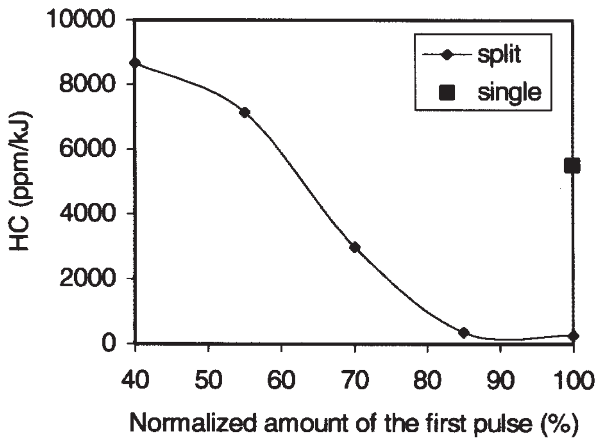

Fig. 20 *Effect of the amount of diesel fuel injected for the first pulse on HC emissions: ϕ_{NG}= 0.33, 1700 r/min.*

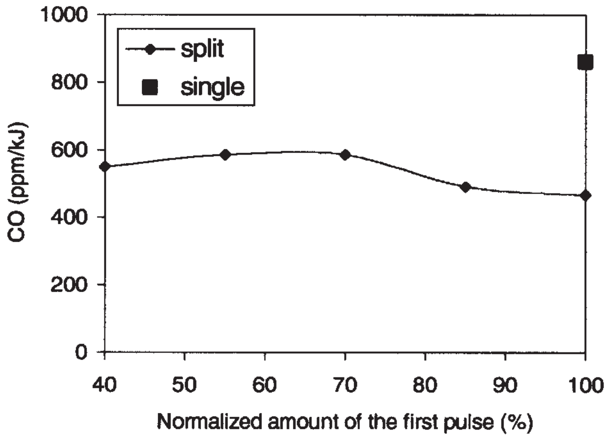

Fig. 21 *Effect of the amount of diesel fuel injected for the first pulse on CO emissions: ϕ_{NG}= 0.33, 1700 r/min.*

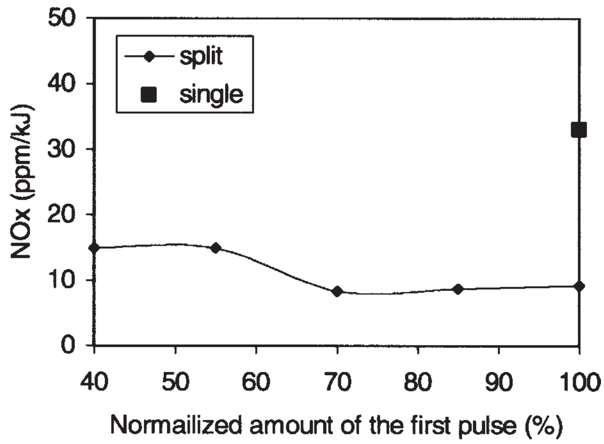

Fig. 22 *Effect of the amount of diesel fuel injected for the first pulse on NO_x emissions: ϕ_{NG}= 0.33, 1700 r/min.*

Therefore, 80–100 per cent of the diesel amount used in the baseline case is recommended.

7. Conclusion

From the current study, it is found that the split diesel injection scheme is a promising method to reduce HC, CO and NO_x emissions at light loads in NG fuelled/micro-pilot ignition engines. It was found that the injection timings of both pulses need to be selected carefully. The optimal timings for the first pulse and the second pulse occur at approximately 260 and 335° CA respectively. With well-selected injection timing, HC emissions can be reduced by more than 90 per cent, while CO production and NO_x production can be reduced by 50 and 70 per cent respectively.

References

1 **O'Neal, G. B.** The diesel-gas dual-fuel engine. In Nonpetroleum Vehicular Fuels Symposium, Paper Nonpetroleum Vehicular Fuels III, 1983, pp. 355–371.

2 **Nichols, R. J.** The challenges of change in the auto industry: why alternative fuels? In *Alternate Fuels, Engine Performance and Emissions*, ICE-Vol. 20, 1993 (American Society of Mechanical Engineers, New York).

3 **Hiltner, J.**, *et al.* HCCI operation with natural gas: fuel composition implications. In ICE Fall Technical Conference, 2000, ICE-Vol. 35-2, Paper 2000-ICE-317.

4 **Kong, S.-C.** and **Reitz, R. D.** Use of detailed chemical kinetics to study HCCI engine combustion with consideration of turbulent mixing effects. In ICE Fall Technical Conference, 2000, ICE-Vol. 35-1, Paper 2000-ICE-306.

5 **Karim, G. A.** The dual fuel engines of compression ignition type—prospects, problems and solutions—a review. SAE Paper 831073, 1983.

6 **Karim, G. A.** The dual fuel engine. In *Automotive Engine Alternatives*, 1987, pp. 83–104 (Plenum Press, New York).

7 **Karim, G. A.** Some considerations of the use of natural gas in diesel engines. In Nonpetroleum Vehicular Fuels Symposium, 1983.

8 **Wong, H. C., Beck, N. J.** and **Chen, S. K.** The evolution of compression ignition natural gas engines for low emission vehicles. In ICE Fall Technical Conference, 2000, ICE-Vol. 35-2, Paper 2000-ICE-318.

9 **Zhang, H., Chiu, J. P.** and **Bartel, J.** Late intake valve closing with throttle control at light loads for a lean-burn natural gas engine. SAE Paper 1999-01-3485, October 1999.

10 **Urata, Y., Umiyama, H., Shimizu, K., Fujiuoshi, Y., Sono, H.** and **Fukuo, K.** A study of vehicle equipped with non-throttling S.I. engine with early intake valve closing mechanism. SAE Paper 930820, 1993.

11 **Khalil, E. B.** and **Karim, G. A.** A kinetic investigation of the role of changes in natural gas composition in relation to gas fuelled engines applications. In ICE Spring Technical Conference, 1997, ICE-Vol. 28-2, Paper 97-ICE-20 (American Society of Mechanical Engineers, New York).

12 **Amsden, A. A.** KIVA-3V: a block-structured KIVA program for engines with vertical or canted valves. Los Alamos National Laboratory Report LA-12503-MS, July 1997.

13 **Chen, J. Y., Westbrook, C. K.** and **Maurice, L. Q.** Reduced chemical kinetic mechanisms for hydrocarbon fuels. In 35th AIAA/ASME/SAE/ASEE Joint Propulsion Conference and Exhibit, Los Angeles, California, June 1999.

14 **Chen, J. Y.** Development of reduced mechanisms for numerical modeling of turbulent combustion. In Workshop on *Numerical Aspects of Reduction in Chemical Kinetics*, CERMICS-ENPC, Cite Descartes-Champus sur Marne, France, 2 September 1997.

15 **Butler, T. D.** Multidimensional numerical simulation of reactive flow in internal combustion engines. *Prog. in Energy and Combust. Sci.*, 1981, **7**, 293–315.

16 **Westbrock, C. K.** and **Dryer, F. L.** Chemical kinetic modelling of hydrocarbon combustion. *Prog. Energy and Combust. Sci.*, 1984, **10**, 1–57.

17 **Dryer, F. L.** and **Glassman, I.** High temperature oxidation of CO and CH_4. In Fourteenth Symposium (International) on *Combustion*, Pittsburgh, Pennsylvania, 1973, p. 987 (The Combustion Institute, Pittsburgh, Pennsylvania).

18 **Heywood, J. B.** *Internal Combustion Engine Fundamentals*, 1988 (McGraw-Hill, New York).

JER 00302